

IEEE Copyright Notice

© 2024 IEEE. Personal use of this material is permitted. Permission from IEEE must be obtained for all other uses, in any current or future media, including reprinting/republishing this material for advertising or promotional purposes, creating new collective works, for resale or redistribution to servers or lists, or reuse of any copyrighted component of this work in other works.

Interference Cancellation for OTFS-Based Over-the-Air Computation

Xinyu Huang*, Henrik Hellström*, and Carlo Fischione*

*Division of Network and Systems Engineering and KTH Digital Futures, KTH Royal Institute of Technology, Sweden

Abstract—This paper investigates over-the-air computation (AirComp) in the context of multiple-access time-varying multipath channels. We focus on a scenario where devices with high mobility transmit their sensing data to a fusion center (FC) for averaging. To combat the time-varying channel and Doppler effect, each device adopts orthogonal time frequency space (OTFS) modulation. After signals are received by the FC, the aggregated data undergoes demodulation and estimation within the delay-Doppler domain. We leverage the mean squared error (MSE) as a metric for the computational error of OTFS-based AirComp. We then derive the optimal transmit power at each device and signal scaling factor at FC for minimizing MSE. Notably, the performance of OTFS-based AirComp is not only affected by the noise but also by the inter-symbol interference and inter-link interference arising from the multipath channel. To counteract the interference-induced computational errors, we incorporate zero-padding (ZP)-assisted OTFS into AirComp and propose algorithms for interference cancellation. Numerical results underscore the enhanced performance of ZP-assisted OTFS-based AirComp over naive OTFS-based AirComp.

Index Terms—Over-the-air computation, orthogonal time frequency space modulation, time-varying channels

I. INTRODUCTION

The Internet of Things (IoT) leads to a pressing challenge of efficient data aggregation from dense networks of devices. The traditional data aggregation method via orthogonal channels becomes highly inefficient due to the restricted spectrum resources. Recently, over-the-air computation (AirComp) was proposed as an efficient method to overcome this issue, which leverages the signal superposition property over the multiple-access channel (MAC) to allow rapid wireless data aggregation [1]. Due to the unique characteristics of AirComp in integrating computation and communication, it is particularly applied in distributed machine learning [2].

Most previous studies, e.g., [2], [3], considered AirComp over time-invariant channels due to the simpler mathematical analysis. However, in the next-generation of wireless networks, there are various emerging applications in high-mobility environments, such as low-earth-orbit (LEO) satellites and high speed trains [4], which lead to a time-varying double-selective channel. Some previous studies, e.g., [5], [6], have investigated AirComp over time-varying channels and estimated the aggregated signal in the time domain. As pre-processing is usually required for AirComp, [5], [6] assumed that the transmitters always know the instantaneous channel gains and the signal estimation is performed within the channel coherence time. This requires frequent signaling with large overhead to broadcast channel state information (CSI) to transmitters.

Also, for fast-varying channels, the channel coherence time can be less than the signaling time, which makes AirComp in [5], [6] potentially impossible. Furthermore, in [7], the authors modulated data via orthogonal frequency-division multiplexing (OFDM). The aggregated signal is estimated on the time frequency domain. However, the high Doppler shifts can generate severe inter-carrier interference, which degrades the performance of OFDM. Also, [7] did not consider any pre-processing or post-processing techniques for reliable AirComp.

To reduce the signaling overhead and eliminate the undesired effects introduced by Doppler shift, orthogonal time frequency space (OTFS) modulation was recently proposed as a promising technique that has been shown to be successful in combating the Doppler effect and time-varying channels [8]. In OTFS, information is modulated on the delay-Doppler domain for transmission, where time-varying channels have almost constant channel gain in the delay-Doppler domain. This advantage transforms designing AirComp over time-varying channels into time-invariant channels, ensuring that the same CSI is utilized for pre-processing of all data. Moreover, channels in the delay-Doppler domain are attributed with compactness and sparsity, which effectively eliminate the inter-carrier interference. Motivated by these advantages, it is worth investigating OTFS for data modulation in AirComp. To the best of the authors' knowledge, OTFS-based AirComp has not been investigated in previous studies.

In this paper, we consider AirComp over multiple-access time-varying channels, where mobile devices simultaneously transmit the sensing data to the fusion center (FC) for averaging. For each device, the data is first modulated on the delay-Doppler domain and then transmitted over the channel. In this paper, we consider a multipath channel between each device and the FC, where different path has different delay and Doppler shifts. We note that the multipath channel was never explicitly considered in previous AirComp studies. After signals are received by the FC, the aggregated signal is also demodulated and estimated on the delay-Doppler domain. Our objective is minimizing the computational error, which is measured by mean squared error (MSE), by jointly optimizing the transmit power at each device and the signal scaling factor, i.e., denoising factor, at the FC. Furthermore, different from the traditional AirComp, the MSE of OTFS-based AirComp is not only influenced by noise but also by inter-symbol interference (ISI) and inter-link interference (ILI) due to the delay and Doppler shifts among multipath channels. To mitigate the

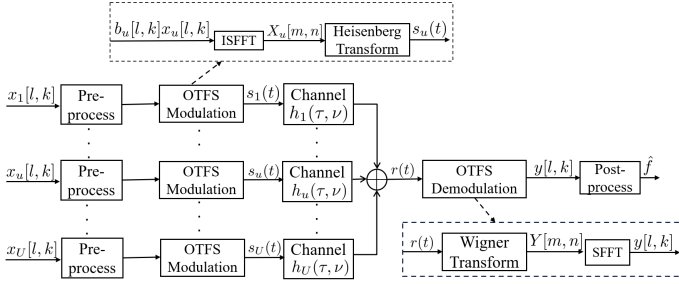


Fig. 1. Illustration of the OTFS-based AirComp system.

impact of interference on the MSE, we further propose using zero-padding (ZP)-assisted OTFS for data modulation, where some null symbols are placed to avoid interference.

The main contributions of this paper can be summarized as follows. First, we derive the closed-form expressions for the optimal transmit power and denoising factor that minimize MSE for OTFS-based AirComp. Second, to further improve the reliability of OTFS-based AirComp, we consider ZP-assisted OTFS for data modulation in AirComp and propose a successive interference cancellation (SIC) algorithm for the averaged data estimation. Numerical results validate the optimality of derived transmit power and denoising factor. They also show that the ZP-assisted OTFS-based AirComp achieves a much lower MSE than OTFS-based AirComp. This efficiency becomes more pronounced with higher signal-to-noise ratio (SNR) and fewer path interferences.

II. SYSTEM MODEL

A. OTFS Modulation & Demodulation

We denote $x_u[l, k] \in \mathbb{C}$ as the transmitted data, which is arranged on the l -th row and k -th column of the delay-Doppler grid for the u -th device. Here, $l \in \{0, 1, \dots, M-1\}$, $k \in \{0, 1, \dots, N-1\}$, and u is any device from the set \mathcal{U} , where M is the number of subcarriers, N is the number of time slots, and $\mathcal{U} = \{1, \dots, U\}$. Then, the total number of data that can be transmitted at each OTFS frame is MN . As in [5], we assume $\mathbb{E}[x_u[l, k]] = 0$, $\mathbb{E}[x_u^2[l, k]] = 1$, and $\mathbb{E}[x_u[l_1, k_1]x_u[l_2, k_2]] = 0, \forall k_1 \neq k_2, l_1 \neq l_2$. A detailed OTFS-based AirComp system that incorporates modulation and demodulation is shown in Fig. 1. We assume that each device and FC are equipped with a single antenna. At the transmitter side, the u -th device first maps $x_u[l, k]$ to $X_u[m, n]$ on the time-frequency domain using the inverse symplectic finite Fourier transform (ISFFT) as

$$X_u[m, n] = \frac{1}{\sqrt{NM}} \sum_{k=0}^{N-1} \sum_{l=0}^{M-1} x_u[l, k] e^{j2\pi(\frac{nk}{N} - \frac{ml}{M})}, \quad (1)$$

where $n = 0, \dots, N-1$ and $m = 0, \dots, M-1$. Then, $X_u[m, n]$ is transformed into a continuous time waveform $s_u(t)$ by the Heisenberg transform [9, Eq. (3)].

The signal $s_u(t)$ is transmitted over a time-varying channel with complex baseband channel impulse response (CIR)

$h_u(\tau, \nu)$, which is given by

$$h_u(\tau, \nu) = \sum_{i=1}^{R_u} h_{u,i} \delta(\tau - \tau_{u,i}) \delta(\nu - \nu_{u,i}), \quad (2)$$

where R_u is the number of propagation paths from the u -th device to FC, $h_{u,i}$, $\tau_{u,i}$, and $\nu_{u,i}$ represent the path gain, delay and Doppler shifts of the i -th path from the u -th device to FC, respectively, and $\delta(\cdot)$ is the Dirac delta function. We further assume that the delay and Doppler shifts are the integer multiples of $1/(M\Delta f)$ and $1/(NT)$, respectively, where NT and $M\Delta f$ are the total duration and bandwidth of one OTFS frame, and we have $T\Delta f = 1$ [10]. Accordingly, we have $\tau_{u,i} = l_{u,i}/(M\Delta f)$ and $\nu_{u,i} = k_{u,i}/(NT)$, where $l_{u,i} \in \mathcal{L}_u$ and $k_{u,i} \in \mathcal{K}_u$ are the indices of delay and Doppler. Here, \mathcal{L}_u and \mathcal{K}_u represent the sets of $l_{u,i}$ and $k_{u,i}$ among all paths between the u -th device and FC. Subsequently, the received signal at the FC is given by

$$r(t) = \sum_{u=1}^U \iint h_u(\tau, \nu) s_u(t - \tau) e^{j2\pi\nu(t - \tau)} d\tau d\nu + w(t), \quad (3)$$

where $w(t)$ is the additive white Gaussian noise (AWGN) at the FC with zero mean and variance σ^2 . At the FC side, $r(t)$ first goes through a matched filter with output $Y(f, t)$, and $Y[m, n]$ is obtained by sampling $Y(f, t)$ at $f = m\Delta f$ and $t = nT$ [9, Eqs. (7), (8)]. Then, $y[l, k]$ is obtained by taking the SFFT on the samples $Y[m, n]$ as

$$y[l, k] = \frac{1}{\sqrt{NM}} \sum_{n=0}^{N-1} \sum_{m=0}^{M-1} Y[m, n] e^{-j2\pi(\frac{nk}{N} - \frac{ml}{M})}. \quad (4)$$

In this paper, we consider a scenario where the pulse shaping filters at the transmitter and receiver adopt rectangular forms. Under this condition, the input-output relationship between $x_u[l, k]$ and $y[l, k]$ is given by [10, Eq. (30)]

$$y[l, k] = \sum_{u=1}^U \sum_{i=1}^{R_u} h_{u,i} \alpha_{u,i}[l, k] \tilde{x}_{u,i} + w[l, k], \quad (5)$$

where $\tilde{x}_{u,i} = x_u[(l - l_{u,i})_M, (k - k_{u,i})_N]$ and

$$\alpha_{u,i}[l, k] = \begin{cases} e^{-j2\pi\frac{k}{N}z^{k_{u,i}}((l-l_{u,i})_M)}, & \text{if } l \leq l_{u,i}, \\ z^{k_{u,i}((l-l_{u,i})_M)}, & \text{if } l \geq l_{u,i}, \end{cases} \quad (6)$$

with $z = e^{j\frac{2\pi}{NM}}$ and $[\cdot]_N$ denotes mod- N operation.

B. OTFS-based AirComp System

From (5), we observe that $y[l, k]$ is a combination of $x_u[l, k]$ that has been shifted according to the delay and Doppler shifts specific to each channel path. Thus, for the corresponding $x_u[l, k]$ to be successfully aggregated at the FC, one successful approach is to designate one path as the principal path. The corresponding $x_u[l, k]$ is then arranged on the delay-Doppler grid in accordance with the delay and Doppler shifts of the principal path for each device. Without any loss of generality, we consider $h_{u,1}, \forall u \in \mathcal{U}$, as the principal path gain. After pre-processing, we multiply $b_u[l, k]$ to each $x_u[l, k]$, where $b_u[l, k]$ is the transmit coefficient. Accordingly, we set $b_u[l, k] = \sqrt{p_u} h_{u,1}^\dagger \alpha_{u,1}^\dagger[l, k] / |h_{u,1}|$, where $p_u \geq 0$ is the transmit power of the u -th device and $h_{u,1}^\dagger$ is the complex conjugate of $h_{u,1}$.

By replacing $x_u[l, k]$ in (5) with $b_u[l, k]x_u[l, k]$, we rephrase (5) as

$$y[l, k] = \sum_{u=1}^U \sqrt{p_u} |h_{u,1}| \tilde{x}_{u,1} + \sum_{u=1}^U \sum_{i=2}^{R_u} \sqrt{p_u} h_{u,i} \times \frac{\alpha_{u,i}[l, k] \alpha_{u,1}^\dagger[l, k] h_{u,1}^\dagger}{|h_{u,1}|} \tilde{x}_{u,i} + w[l, k]. \quad (7)$$

In (7), we observe that only the time-invariant path gain, delay shift, and Doppler shift of the principal path are required for pre-processing at each device, instead of instantaneous CSI. Moreover, we observe that compared to the conventional input-output relationship of the AirComp system, the OTFS-based AirComp system suffers from additional ISI and ILI from other devices, which are caused by the delay and Doppler spread of multipath channels. In this paper, our aim is to estimate the average of the transmitted values from devices, i.e., $f[l, k] = \sum_{u=1}^U \tilde{x}_{u,1}/U, \forall l \in \{1, \dots, M-1\}, k \in \{1, \dots, N-1\}$. We note that the arrangement of $x_u[l, k]$ is based on $l_{u,1}$ and $k_{u,1}$ such that the corresponding $x_u[l, k]$ can be added together. After obtaining $y[l, k]$, the FC estimates $f[l, k]$ as $\hat{f}[l, k] = y[l, k]/(U\sqrt{\eta})$, where $\eta \geq 0$ is the denoising factor. We further denote ϵ as the mean-squared error (MSE) between $\hat{f}[l, k]$ and $f[l, k]$, which is given by

$$\epsilon = \frac{1}{U^2} \mathbb{E} \left[\left(\frac{y[l, k]}{\sqrt{\eta}} - \sum_{u=1}^U \tilde{x}_{u,1} \right)^2 \right], \quad (8)$$

where the expectation is taken over $x_u[l, k]$ and noise. By substituting (7) into (8), we obtain

$$\epsilon = \sum_{u=1}^U \left(\frac{\sqrt{p_u} |h_{u,1}|}{\sqrt{\eta}} - 1 \right)^2 + \sum_{u=1}^U \sum_{i=2}^{R_u} \frac{p_u |h_{u,i}|^2}{\eta} + \frac{\sigma^2}{\eta}, \quad (9)$$

where we omit $1/U^2$ for simplicity.

III. OTFS-BASED AIRCOMP DESIGN

In this section, we jointly optimize the transmit power p_u and denoising factor η to minimize the MSE defined in (9). Assuming each user operates under an average power budget denoted by P , we formulate the optimization problem, referred to as $\mathcal{P}1$, as follows

$$\mathcal{P}1 : \min_{p_u \geq 0, \eta \geq 0} \sum_{u=1}^U \left(\frac{\sqrt{p_u} |h_{u,1}|}{\sqrt{\eta}} - 1 \right)^2 + \sum_{u=1}^U \sum_{i=2}^{R_u} \frac{p_u |h_{u,i}|^2}{\eta} + \frac{\sigma^2}{\eta}, \quad (10)$$

s.t. $p_u \leq P, \forall u \in \mathcal{U}$.

We first optimize p_u for any given $\eta \geq 0$. Accordingly, $\mathcal{P}1$ is simplified as

$$\min_{p_u \geq 0} \sum_{u=1}^U \left(\frac{\sqrt{p_u} |h_{u,1}|}{\sqrt{\eta}} - 1 \right)^2 + \sum_{u=1}^U \sum_{i=2}^{R_u} \frac{p_u |h_{u,i}|^2}{\eta}, \quad (11)$$

s.t. $p_u \leq P, \forall u \in \mathcal{U}$.

By taking the derivative of (11) with respect to p_u , we calculate the optimal p_u , denoted by \hat{p}_u , that minimizes (11) without accounting for the power constraint as $\hat{p}_u = |h_{u,1}|^2 \eta / (\sum_{i=1}^{R_u} |h_{u,i}|^2)^2$. Upon incorporating the power constraint, the optimal transmit power, denoted by p_u^* , is given

$$p_u^* = \min \left(P, \frac{|h_{u,1}|^2 \eta}{\left(\sum_{i=1}^{R_u} |h_{u,i}|^2 \right)^2} \right). \quad (12)$$

We then optimize η . By substituting (12) into (10), we obtain the following optimization problem, denoted by $\mathcal{P}2$, as

$$\mathcal{P}2 : \min_{\eta \geq 0} \sum_{u=1}^U \left(\min \left(\frac{\sqrt{P} |h_{u,1}|}{\sqrt{\eta}}, \frac{|h_{u,1}|^2}{\sum_{i=1}^{R_u} |h_{u,i}|^2} \right) - 1 \right)^2 + \sum_{u=1}^U \sum_{i=2}^{R_u} \min \left(\frac{P |h_{u,i}|^2}{\eta}, \left(\frac{|h_{u,1}| |h_{u,i}|}{\sum_{i=1}^{R_u} |h_{u,i}|^2} \right)^2 \right) + \frac{\sigma^2}{\eta}. \quad (13)$$

Without loss of generality, we assume that

$$\frac{\sum_{i=1}^{R_1} |h_{1,i}|^2}{|h_{1,1}|} \leq \dots \leq \frac{\sum_{i=1}^{R_u} |h_{u,i}|^2}{|h_{u,1}|} \leq \dots \leq \frac{\sum_{i=1}^{R_U} |h_{U,i}|^2}{|h_{U,1}|}. \quad (14)$$

To solve $\mathcal{P}2$, we divide the value of η into $U+1$ intervals and define the u -th interval, $\forall u \in \{0, \mathcal{U}\}$, as

$$I_u = \left\{ \eta \left| P \left(\frac{\sum_{i=1}^{R_u} |h_{u,i}|^2}{|h_{u,1}|} \right)^2 \leq \eta \leq P \left(\frac{\sum_{i=1}^{R_{u+1}} |h_{u+1,i}|^2}{|h_{u+1,1}|} \right)^2 \right\}, \quad (15)$$

where we define $\sum_{i=1}^{R_0} |h_{0,i}|^2 / |h_{0,1}| = 0$ and $\sum_{i=1}^{R_{U+1}} |h_{U+1,i}|^2 / |h_{U+1,1}| = \infty$. Then, for $\eta \in I_u$, $\mathcal{P}2$ can be rephrased as

$$\min_{\eta \in I_u} H_u(\eta) = \sum_{j=1}^u \left(\frac{\sqrt{P} |h_{j,1}|}{\sqrt{\eta}} - 1 \right)^2 + \sum_{j=u+1}^U \left(\frac{|h_{j,1}|^2}{\sum_{i=1}^{R_j} |h_{j,i}|^2} - 1 \right)^2 + \sum_{j=1}^u \sum_{i=2}^{R_j} \frac{P |h_{j,i}|^2}{\eta} + \sum_{j=u+1}^U \sum_{i=2}^{R_j} \frac{|h_{j,1}|^2 |h_{j,i}|^2}{\left(\sum_{i=1}^{R_u} |h_{u,i}|^2 \right)^2} + \frac{\sigma^2}{\eta}. \quad (16)$$

We denote $\hat{\eta}_u > 0$ as the optimal η that achieves the minimum $H_u(\eta)$, where $H_u(\eta)$ first decreases on $[0, \hat{\eta}_u]$, and then increases on $[\hat{\eta}_u, \infty]$. By computing $\partial H_u(\eta) / \partial \eta = 0$, we obtain $\hat{\eta}_u$ as

$$\hat{\eta}_u = \left(\frac{\sum_{j=1}^u \sum_{i=1}^{R_j} P |h_{j,i}|^2 + \sigma^2}{\sum_{j=1}^u \sqrt{P} |h_{j,1}|} \right)^2. \quad (17)$$

We then denote $\eta_u^* \in I_u$ as the optimal η that minimizes (16). According to (15) and (17), η_u^* is given by

$$\eta_u^* = \min \left[P \left(\frac{\sum_{i=1}^{R_{u+1}} |h_{u+1,i}|^2}{|h_{u+1,1}|} \right)^2, \max \left(\hat{\eta}_u, P \left(\frac{\sum_{i=1}^{R_u} |h_{u,i}|^2}{|h_{u,1}|} \right)^2 \right) \right]. \quad (18)$$

We further denote η^* as the optimal η for $\mathcal{P}2$, which can be determined by comparing the values of $H_u(\eta_u^*)$ for η_u^* within each interval. We suppose that $\eta^* = \eta_{u^*}^*$ and obtain $u^* = \arg \min_{u \in \mathcal{U}} H_u(\eta_u^*)$. Then, based on (12), (15), and (18), we derive and present p_u^* and η^* in the following theorem.

Theorem 1: The optimal p_u and η that jointly minimize $\mathcal{P}1$ are given by

$$p_u^* = \begin{cases} P, \forall u \in \{1, \dots, u^*\}, \\ \frac{|h_{u,1}|^2 \eta^*}{\left(\sum_{i=1}^{R_u} |h_{u,i}|^2 \right)^2}, \forall u \in \{u^* + 1, \dots, U\}, \end{cases} \quad (19)$$

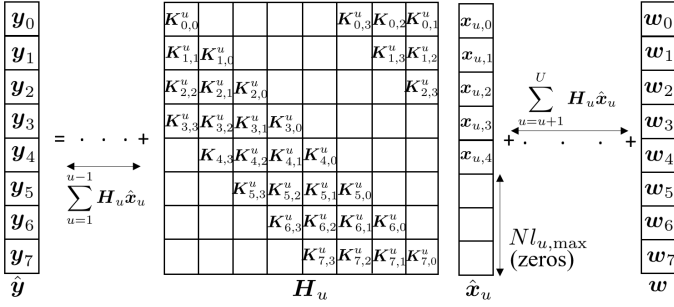


Fig. 2. Delay-Doppler domain input-output relation for $N = M = 8$, $R_u = 4$, $l_u = [0, 1, 2, 3]$, and $k_u = [0, 1, 2, 3]$, $\forall u \in \mathcal{U}$.

and

$$\eta^* = \left(\frac{\sum_{j=1}^{u^*} \sum_{i=1}^{R_j} P |h_{j,i}|^2 + \sigma^2}{\sum_{j=1}^{u^*} \sqrt{P} |h_{j,1}|} \right)^2. \quad (20)$$

Proof: The proof of Theorem 1 is similar to [5, Appendix C], and we omit the details here due to the page limit. ■

IV. SIC FOR ZP-ASSISTED OTFS-BASED AIRCOMP

In this section, we introduce the ZP-assisted OTFS and investigate its application in AirComp. We propose a novel algorithm for the ZP-assisted OTFS-based AirComp framework, which applies the SIC during aggregated signal estimation at the FC. In this algorithm, we optimize the transmit power, the denoising factor, and a coefficient for interference cancellation.

A. ZP-Assisted OTFS

We denote $\mathbf{X}_u \in \mathbb{C}^{M \times N}$ and $\mathbf{Y} \in \mathbb{C}^{M \times N}$ as the two-dimensional (2D) transmitted and received data matrices in the delay-Doppler grid, respectively. In [11], the authors proposed ZP-assisted OTFS, where the data in the last $l_{u,\max}$ rows of \mathbf{X}_u are set to zero to avoid inter-block interference in the time domain. Here, $l_{u,\max}$ is the maximum channel delay spread index between the u -th device and FC. We further denote $\mathbf{x}_{u,m} \in \mathbb{C}^{N \times 1}$ and $\mathbf{y}_m \in \mathbb{C}^{N \times 1}$ as the column vectors that contain the data in the m -th row of \mathbf{X}_u and \mathbf{Y} , respectively, i.e., $\mathbf{x}_{u,m} = [\mathbf{X}_u[m, 0], \mathbf{X}_u[m, 1], \dots, \mathbf{X}_u[m, N-1]]^T$ and $\mathbf{y}_m = [\mathbf{Y}[m, 0], \mathbf{Y}[m, 1], \dots, \mathbf{Y}[m, N-1]]^T$. We denote $\hat{\mathbf{x}}_u \in \mathbb{C}^{NM \times 1}$ and $\hat{\mathbf{y}} \in \mathbb{C}^{NM \times 1}$ as the vectors of the transmitted data at the u -th device and the received data at the FC, respectively, where $\hat{\mathbf{y}} = [\mathbf{y}_0^T, \mathbf{y}_1^T, \dots, \mathbf{y}_{M-1}^T]^T$ and $\hat{\mathbf{x}}_u = [\mathbf{x}_{u,0}^T, \mathbf{x}_{u,1}^T, \dots, \mathbf{x}_{u,M-1}^T]^T$. According to [11, Eq. (30)], the relationship between $\hat{\mathbf{x}}_u$ and $\hat{\mathbf{y}}$ is $\hat{\mathbf{y}} = \sum_{u=1}^U \mathbf{H}_u \hat{\mathbf{x}}_u + \mathbf{w}$, where $\mathbf{H}_u \in \mathbb{C}^{MN \times MN}$ is the channel matrix between the u -th device and FC in the delay-Doppler domain and \mathbf{w} is the AWGN vector with zero mean and variance σ^2 for each element. In Fig. 2, we show a configuration example, where $\mathbf{K}_{m,l}^u \in \mathbb{C}^{N \times N}$ within \mathbf{H}_u for $l \in \mathcal{L}_u$. According to [11], $\mathbf{K}_{m,l}^u$ is given by $\mathbf{K}_{m,l}^u = \text{circ}[\nu_{m,l}^u(0), \dots, \nu_{m,l}^u(N-1)]$, where $\text{circ}[\cdot]$ is the circulant matrix and $\nu_{m,l}^u(\kappa) = \begin{cases} h_{u,i} z^{k(m-l)}, & \text{if } l = l_{u,i}, k = k_{u,i}, \text{ and } \kappa = [k_{u,i}]_N, \\ 0, & \text{otherwise.} \end{cases}$

(21)

From Fig. 2, it is evident that the configuration of \mathbf{H}_u is influenced by both the number of channel paths and the respective delay and Doppler shifts within each path. To ensure an accurate aggregation of $\hat{\mathbf{x}}_u$ and effective SIC, we assume that $h_u(\tau, \nu)$, $\forall u \in \mathcal{U}$, has an identical number of paths, as well as consistent delay and Doppler shifts in each of those paths, i.e., $R_1 = \dots = R_U = R$, $l_{1,i} = \dots = l_{U,i} = l_i$, and $k_{1,i} = \dots = k_{U,i} = k_i$.

B. Algorithm for Interference Cancellation

As the last Nl_{\max} elements in $\hat{\mathbf{x}}_u$ are always set as zero as shown in Fig. 2, $\sum_{u=1}^U \mathbf{x}_{u,0}$ and $\sum_{u=1}^U \mathbf{x}_{u,M-l_{\max}-1}$ can always be estimated without any interference. Moreover, as the estimation of $\sum_{u=1}^U \mathbf{x}_{u,2}$ in Fig. 2 experiences the most interference, its estimation is deferred to the last position. Therefore, a prioritized sequence for estimating $\sum_{u=1}^U \mathbf{x}_{u,m}$, $\forall m \in \{0, \dots, M-l_{\max}-1\}$, is $[\mathbf{x}_{u,0}, \mathbf{x}_{u,1}, \dots, \mathbf{x}_{u,m^*}, \mathbf{x}_{u,M-l_{\max}-1}, \mathbf{x}_{u,M-l_{\max}-2}, \dots, \mathbf{x}_{u,m^*+1}]$, where m^* is determined by delays among all paths. The process for determining m^* is described in following remark.

Remark 1: We apply integer θ_m to measure the level of impact of the interference on the estimation of $\sum_{u=1}^U \mathbf{x}_{u,m}$. For the estimation of $\sum_{u=1}^U \mathbf{x}_{u,m_1}$, the interference is either within the interval $[\mathbf{x}_{u,0}, \mathbf{x}_{u,m_1-1}]$ or within $[\mathbf{x}_{u,m_1+1}, \mathbf{x}_{u,M-l_{\max}-1}]$. When the interference is within $[\mathbf{x}_{u,0}, \mathbf{x}_{u,m_1-1}]$, we set $\theta_{m_1} = \theta_{m_1}^+$, and assume that there are $|\mathcal{M}^+|$ interferences $\mathbf{x}_{u,m}$, $\forall m \in \mathcal{M}^+$, where \mathcal{M}^+ is a set containing the index m of all interference terms within $[\mathbf{x}_{u,0}, \mathbf{x}_{u,m_1-1}]$. When the interference is within $[\mathbf{x}_{u,m_1+1}, \mathbf{x}_{u,M-l_{\max}-1}]$, we set $\theta_{m_1} = \theta_{m_1}^-$, and assume that there are $|\mathcal{M}^-|$ interferences $\mathbf{x}_{u,m}$, $\forall m \in \mathcal{M}^-$. Then, we calculate $\theta_{m_1}^+$ and $\theta_{m_1}^-$ as $\theta_{m_1}^+ = \sum_{m \in \mathcal{M}^+} \theta_m^+ + |\mathcal{M}^+|$ and $\theta_{m_1}^- = \sum_{m \in \mathcal{M}^-} \theta_m^- + |\mathcal{M}^-|$. When there is no interference for estimation, we set $\theta_{m_1}^+ = \theta_{m_1}^- = 0$. After obtaining $\theta_{m_1}^+$ and $\theta_{m_1}^-$, m^* is determined as the minimum m_1 when $\theta_{m_1}^+ \leq \theta_{m_1}^-$.

We consider the scenario that l_i on each path is different, i.e., $l_i \neq l_j, \forall i \neq j, 1 \leq i, j \leq R$.¹ Then, only one element in each row of $\mathbf{K}_{m,l}^u$ is non-zero. We first consider the scenario with *no interference* during the estimation of $\sum_{u=1}^U \mathbf{x}_{u,m}$. To illustrate this, we use the estimation of $\sum_{u=1}^U \mathbf{x}_{u,0}$ from Fig. 2 as an example. We define $\gamma_m \in \{mN, \dots, (m+1)N-1\}$ and denote y_{γ_m} , x_{u,γ_m} , and w_{γ_m} as the γ_m th element in $\hat{\mathbf{y}}$, $\hat{\mathbf{x}}_u$, and \mathbf{w} , respectively. As only $\nu_{0,0}^u(0) = h_{u,1}$ in $\mathbf{K}_{0,0}^u$ is non-zero, the relationship between y_{γ_0} and x_{u,γ_0} is given by

$$y_{\gamma_0} = \sum_{u=1}^U \sqrt{p_{u,0}} |h_{u,1}| x_{u,\gamma_0} + w_{\gamma_0}, \quad (22)$$

where $\sqrt{p_{u,m}}$ is the transmit power for x_{u,γ_m} . We denote $\hat{f}_{m_1} = y_{\gamma_{m_2}} / \sqrt{\eta_{m_2}}$ as the estimated value of $\sum_{u=1}^U x_{u,\gamma_{m_1}}$ and ϵ_{m_1} as the MSE associated with estimating $\sum_{u=1}^U x_{u,\gamma_{m_1}}$, where η_{m_2} is the denoising factor for $y_{\gamma_{m_2}}$. We note that (22) has a same format as that of [5, Eq. (5)], which suggests that the

¹The scenario that at least two paths share the same delay will be investigated in the extended version.

optimization procedures of $p_{u,0}$ and η_0 can follow [5]. Thus, $p_{u,0}^*$ and η_0^* are given by [5, Eqs. (24), (25)]

$$p_{u,0}^* = \begin{cases} P, \forall u \in \{1, \dots, u_0^*\}, \\ \frac{\eta_0^*}{|h_{u,1}|^2}, \forall u \in \{u_0^* + 1, \dots, U\}, \end{cases} \quad (23)$$

and

$$\eta_0^* = \left(\frac{\sigma^2 + \sum_{j=1}^{u_0^*} P|h_{j,1}|^2}{\sum_{j=1}^{u_0^*} \sqrt{P}|h_{j,1}|} \right)^2, \quad (24)$$

respectively, with $u_0^* = \min_u \left(\frac{\sigma^2 + \sum_{j=1}^u P|h_{j,1}|^2}{\sum_{j=1}^u \sqrt{P}|h_{j,1}|} \right)^2$.

Next, we consider the scenario where multiple interferences impact the estimation of $\sum_{u=1}^U x_{u,m}$. For illustrative purposes, we focus on the estimation of $\sum_{u=1}^U x_{u,1}$ as an example. As depicted in Fig. 2, x_{u,γ_0} acts as an interference during the estimation of $\sum_{u=1}^U x_{u,\gamma_1}$ when examining the relationship between x_{u,γ_1} and y_{γ_1} . Given that we have estimated $\sum_{u=1}^U x_{u,\gamma_0}$, it can be subtracted from y_{γ_1} , leading to

$$y_{\gamma_1} = \sum_{u=1}^U \sqrt{p_{u,1}} |h_{u,1}| x_{u,\gamma_1} + \sum_{u=1}^U \frac{\sqrt{p_{u,0}^*} h_{u,2} h_{u,1}^\dagger}{|h_{u,1}|} x_{u,\gamma_0} + w_{\gamma_1} - \zeta_{1,0} \hat{f}_0, \quad (25)$$

where $\zeta_{m,j} > 0$ is a coefficient for \hat{f}_j subtracted from the signal y_{γ_m} . By substituting (25) and \hat{f}_0 into (8), we formulate the optimization problem that minimizes the MSE between \hat{f}_1 and $\sum_{u=1}^U x_{u,\gamma_1}/U$ as

$$\mathcal{P3}: \min_{p_{u,1} \geq 0, \eta_1 \geq 0, \zeta_{1,0} \geq 0} \epsilon_1 = \sum_{u=1}^U \left(\frac{p_{u,1} |h_{u,1}|}{\sqrt{\eta_1}} - 1 \right)^2 + \frac{\mathbb{E}[G(\zeta_{1,0})^2]}{\eta_1}, \text{ s.t. } p_{u,1} \leq P, \forall u \in \mathcal{U}, \quad (26)$$

where

$$G(\zeta_{1,0}) = \sum_{u=1}^U \left(\frac{h_{u,2} \sqrt{p_{u,0}^*} h_{u,1}^\dagger}{|h_{u,1}|} - \frac{\zeta_{1,0} \sqrt{p_{u,0}^*} |h_{u,1}|}{\sqrt{\eta_0^*}} \right) x_{u,\gamma_0} + w_{\gamma_1} - \frac{\zeta_{1,0} w_{\gamma_0}}{\sqrt{\eta_0^*}}. \quad (27)$$

In the following theorem, we derive and present the optimal $p_{u,1}$, η_1 , and $\zeta_{1,0}$ for $\mathcal{P3}$.

Theorem 2: The optimal $p_{u,1}$, η_1 , and $\zeta_{1,0}$ that jointly minimize $\mathcal{P3}$ are given by

$$p_{u,1}^* = \begin{cases} P, \forall k \in \{1, \dots, u_1^*\}, \\ \frac{\eta_1^*}{|h_{u,1}|^2}, \forall u \in \{u_1^* + 1, \dots, U\}, \end{cases} \quad (28)$$

$$\eta_1^* = \left(\frac{\min \mathbb{E}[G(\zeta_{1,0})^2] + \sum_{j=1}^{u_1^*} P|h_{j,1}|^2}{\sum_{j=1}^{u_1^*} \sqrt{P}|h_{j,1}|} \right)^2, \quad (29)$$

and

$$\zeta_{1,0}^* = \frac{\sqrt{\eta_1^*} \sum_{u=1}^U |h_{u,2}| |h_{u,1}| p_{u,0}^*}{\sum_{u=1}^U p_{u,0}^* |h_{u,1}|^2 + \sigma^2}, \quad (30)$$

where

$$\min \mathbb{E}[G(\zeta_{1,0})^2] = \sum_{u=1}^U |h_{u,2}|^2 p_{u,0}^* + \sigma^2 - \frac{(\sum_{u=1}^U |h_{u,2}| |h_{u,1}| p_{u,0}^*)^2}{\sum_{u=1}^U p_{u,0}^* |h_{u,1}|^2 + \sigma^2}, \quad (31)$$

and

$$u_1^* = \min_u \left(\frac{\min \mathbb{E}[G(\zeta_{1,0})^2] + \sum_{j=1}^u P|h_{j,1}|^2}{\sum_{j=1}^u \sqrt{P}|h_{j,1}|} \right)^2. \quad (32)$$

Proof: Please see Appendix A. ■

Notably, the estimation of $\sum_{u=1}^U x_{u,\gamma_1}$ in (25) is influenced only by a single interference x_{u,γ_0} . Furthermore, we consider the scenario that the detection of $\sum_{u=1}^U x_{u,\gamma_{m_1}}$ is affected by more than one interference, denoted by x_{γ_m} , $\forall m \in \mathcal{M}$, where \mathcal{M} represents the set for the index m of the interference. Under this scenario, the relationship between $x_{u,\gamma_{m_1}}$ and $y_{\gamma_{m_2}}$ is given by

$$y_{\gamma_{m_2}} = \sum_{u=1}^U \sqrt{p_{u,m_1}} |\nu_{m_2,l}^u| x_{u,\gamma_{m_1}} + \sum_{m \in \mathcal{M}} \sum_{u=1}^U \sqrt{p_{u,m}^*} \nu_{m_2,m_1-m+l}^u \times \frac{(\nu_{m_2,l}^u)^\dagger x_{u,\gamma_m}}{|\nu_{m_2,l}^u|} + w_{\gamma_{m_2}} - \sum_{m \in \mathcal{M}} \zeta_{m_2,m} \hat{f}_m, \quad (33)$$

where ν_{m_2,m_1-m+l}^u represents the non-zero element in $\mathbf{K}_{m_2,m_1-m+l}^u$ that corresponds to x_{u,γ_m} . Here, $y_{\gamma_{m_2}}$ is chosen to result in a minimum θ_{m_1} for $x_{u,\gamma_{m_1}}$. We then formulate the optimization problem based on the MSE between \hat{f}_{m_1} and $\sum_{u=1}^U x_{u,\gamma_{m_1}}/U$ as

$$\min_{p_{u,m_1} \geq 0, \eta_{m_2} \geq 0, \zeta_{m_2,m} \geq 0, \forall m \in \mathcal{M}} \epsilon_{m_1} = \sum_{u=1}^U \left(\frac{\sqrt{p_{u,m_1}} |\nu_{m_2,l}^u|}{\sqrt{\eta_{m_2}}} - 1 \right)^2 + \frac{\sum_{m \in \mathcal{M}} \mathbb{E}[G(\zeta_{m_2,m})^2]}{\eta_{m_2}}, \text{ s.t. } p_{u,m_1} \leq P, \forall u \in \mathcal{U}, \quad (34)$$

where $E[G(\zeta_{m_2,m})^2]$ is the quadratic function relating to $\zeta_{m_2,m}$. Since (34) has a same format as that of (26), optimal values p_{u,m_1}^* , $\eta_{m_2}^*$, and $\zeta_{m_2,m}^*$ can be derived accordingly, as shown in Appendix A.

V. NUMERICAL RESULTS

In this section, we evaluate the MSE performance of both OTFS-based AirComp and ZP-assisted OTFS-based AirComp. The analysis focuses on the average MSE over a large number of channel realizations. Specifically, we set $M = 32$, $N = 16$, $U = 20$, $R_u = 4$, unless otherwise stated. The path gains are randomly generated based on a uniform power delay profile, and the delay and Doppler indices are randomly generated within the range of $[0, l_{\max}]$ and $[-k_{\max}, k_{\max}]$, where $l_{\max} = 10$ and $k_{\max} = 5$ [12]. During the simulation, we always assume that $l_{u,1} \leq l_{u,2} \leq \dots \leq l_{u,R_u}$.

In Fig. 3, we plot MSE versus SNR for OTFS-based AirComp and ZP-assisted OTFS-based AirComp, where SNR is defined as P/σ^2 . First, we apply different transmission power policies for OTFS-based AirComp. Our observations reveal that assigning optimal transmit power according to Theorem 1 results in a lower MSE compared to allotting full transmit power to all devices or to a singular device. This supports the optimal efficiency of p_u^* and η^* in minimizing MSE. Second, we observe that an MSE plateaus of OTFS-based AirComp for larger SNR, which reveals the fact that interference plays the pivotal role in degrading the performance of computation. We further observe that MSE for ZP-assisted OTFS-based

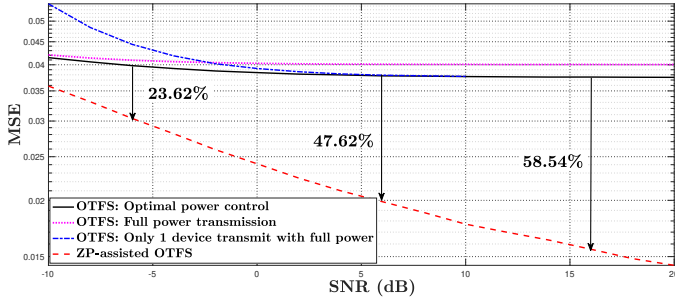


Fig. 3. MSE versus SNR for OTFS-based AirComp and ZP-assisted OTFS-based AirComp, where different transmission power policies are applied.

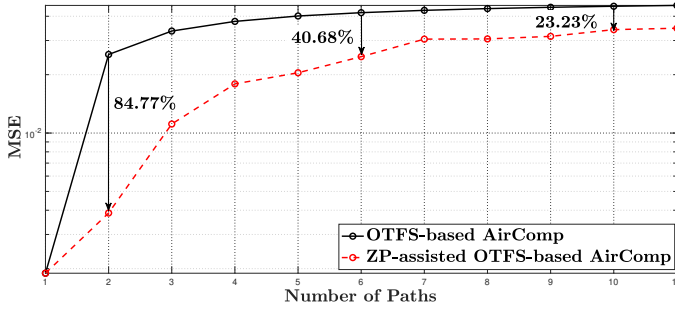


Fig. 4. MSE versus number of paths for OTFS-based AirComp and ZP-assisted OTFS-based AirComp, where SNR = 10 dB.

AirComp is much lower than that of OTFS-based AirComp, which proves the superiority of ZP-assisted OTFS in mitigating the impact of interference. We also show that the superiority becomes more obvious as SNR increases.

In Fig. 4, we depict the MSE versus the number of channel paths for both OTFS-based AirComp and ZP-assisted OTFS-based AirComp. First, our observations indicate that the MSEs for both systems increase with the increase in the number of paths. This is due to the fact that a larger number of paths introduces more interferences. Second, the gap between MSEs for both systems decreases as the number of paths increases, which demonstrates that the algorithm in Section IV-B is more proficient in mitigating interference impacts when the number of channel paths is small.

VI. CONCLUSION

In this paper, we investigated OTFS-based AirComp over double-selective time-varying channels, where devices modulate data in the delay-Doppler domain before transmitting it to the FC. We derived the optimal transmit power and denoising factor that achieve the minimum MSE for the estimation of the averaged data at FC. Due to the existence of interference in OTFS-based AirComp, we further applied ZP-assisted OTFS at each device and proposed an algorithm that can effectively mitigate the interference. Numerical results showed that the performance of OTFS-based AirComp is mainly impacted by interference and that applying ZP-assisted OTFS can achieve a much lower MSE. In future research, we will integrate channel estimation into OTFS-based AirComp.

APPENDIX A PROOF OF THEOREM 2

We first derive $\zeta_{1,0}^*$. From (26), we can see that only $\mathbb{E}[G(\zeta_{1,0})^2]$ relates to $\zeta_{1,0}$. Therefore, we need to find $\zeta_{1,0}^*$ that minimizes $\mathbb{E}[G(\zeta_{1,0})^2]$. We note that the expectation of $G(\zeta_{1,0})$ is taken over x_{u,γ_0} , w_{γ_1} , and w_{γ_0} . As x_{u,γ_0} , w_{γ_1} , and w_{γ_0} are independent with each other, $\mathbb{E}[G(\zeta_{1,0})^2]$ is derived as

$$\mathbb{E}[G(\zeta_{1,0})^2] = \frac{\sum_{u=1}^U p_{u,0}^* |h_{u,1}|^2 + \sigma^2}{\eta_0^*} \zeta_{1,0}^2 - \frac{2 \sum_{u=1}^U |h_{u,2}| |h_{u,1}| p_{u,0}^*}{\sqrt{\eta_0^*}} \zeta_{1,0} + \sum_{u=1}^U |h_{u,2}|^2 p_{u,0}^* + \sigma^2. \quad (35)$$

Since (35) is a quadratic function, the optimal $\zeta_{1,0}^*$ can be obtained by calculating $\partial \mathbb{E}[G(\zeta_{1,0})^2] / \partial \zeta_{1,0} = 0$, which leads to (30). By substituting $\zeta_{1,0}^*$ into (35), we can obtain $\min \mathbb{E}[G(\zeta_{1,0})^2]$. After obtaining $\zeta_{1,0}^*$, the optimization problem in (26) becomes

$$\min_{p_{u,1} \geq 0, \eta_1 \geq 0} \epsilon_1 = \sum_{u=1}^U \left(\frac{p_{u,1} |h_{u,1}|}{\sqrt{\eta_1}} - 1 \right)^2 + \frac{\min \mathbb{E}[G(\zeta_{1,0})^2]}{\eta_1}, \quad \text{s.t. } p_{u,1} \leq P. \quad (36)$$

We note that the optimization problem in (36) is the same as the problem for estimating $\sum_{u=1}^U x_{u,\gamma_0}$ in (22). Then, (28) and (29) can be obtained following (23) and (24), respectively.

ACKNOWLEDGEMENT

The work was supported by the following projects: KAW TAIRCOMP, SSF SAICOM, and DF DEMOCRITUS.

REFERENCES

- [1] A. Şahin and R. Yang, "A survey on over-the-air computation," *IEEE Commun. Surv. Tutor.*, vol. 25, no. 3, pp. 1877–1908, 3rd Quart. 2023.
- [2] K. Yang, T. Jiang, Y. Shi, and Z. Ding, "Federated learning via over-the-air computation," *IEEE Trans. Wireless Commun.*, vol. 19, no. 3, pp. 2022–2035, Mar. 2020.
- [3] G. Zhu and K. Huang, "MIMO over-the-air computation for high-mobility multimodal sensing," *IEEE Internet Things J.*, vol. 6, no. 4, pp. 6089–6103, Aug. 2018.
- [4] W. Saad, M. Bennis, and M. Chen, "A vision of 6G wireless systems: Applications, trends, technologies, and open research problems," *IEEE Netw.*, vol. 34, no. 3, pp. 134–142, May 2019.
- [5] X. Cao, G. Zhu, J. Xu, and K. Huang, "Optimized power control for over-the-air computation in fading channels," *IEEE Trans. Wirel. Commun.*, vol. 19, no. 11, pp. 7498–7513, Nov. 2020.
- [6] M. Fu, Y. Zhou, Y. Shi, T. Wang, and W. Chen, "UAV-assisted over-the-air computation," in *IEEE ICC 2021*, Montreal, QC, Canada, Jun. 2021, pp. 1–6.
- [7] B. Tegin and T. M. Duman, "Federated learning with over-the-air aggregation over time-varying channels," *IEEE Trans. Wirel. Commun.*, vol. 22, no. 8, Aug. 2023.
- [8] R. Hadani *et al.*, "Orthogonal time frequency space modulation," in *IEEE WCNC 2017*, San Francisco, CA, USA, Mar. 2017, pp. 1–6.
- [9] P. Raviteja *et al.*, "Interference cancellation and iterative detection for orthogonal time frequency space modulation," *IEEE Trans. Wirel. Commun.*, vol. 17, no. 10, pp. 6501–6515, Oct. 2018.
- [10] P. Raviteja, Y. Hong, E. Viterbo, and E. Biglieri, "Practical pulse-shaping waveforms for reduced-cyclic-prefix OTFS," *IEEE Trans. Veh. Technol.*, vol. 68, no. 1, pp. 957–961, Jan. 2018.
- [11] T. Thaj and E. Viterbo, "Low complexity iterative rake decision feedback equalizer for zero-padded OTFS systems," *IEEE Trans. Veh. Technol.*, vol. 69, no. 12, pp. 15 606–15 622, Dec. 2020.
- [12] S. Li, W. Yuan, Z. Wei, and J. Yuan, "Cross domain iterative detection for orthogonal time frequency space modulation," *IEEE Trans. Wirel. Commun.*, vol. 21, no. 4, pp. 2227–2242, Apr. 2021.